Digital timing in positron emission tomography

Pedro Guerra *IEEE Graduate Member*, Juan E. Ortuño, George Kontaxakis *IEEE Senior Member*, Maria J. Ledesma *IEEE Member*, Juan J. Vaquero *IEEE Senior Member*, Manuel Desco and Andres Santos *IEEE Senior Member*

***Abstract*– Positron emission tomography (PET) requires accurate timing of events in order to properly discriminate between coincident and non-coincident events. The traditional solution to timing is based on custom ASIC designs, whose cost may not be justified in the design of an experimental small animal PET scanner. The new generation of PET scanners introduces the idea of continuous sampling of the detected scintillation pulse, in substitution of the event triggered acquisition systems. This approach enables new options to timing based on digital processing of the sampled pulse signal. This work proposes a time stamping algorithm based on the optically matched filter and compares the potential performance benefits of this approach versus other FIR filter designs, some of which have been already implemented by different authors. Results show that time resolution of the timestamp may be as 1 ns without the need of expensive high-speed converters when the proper processing is applied.**

Keywords: PET front-end, digital timing

I. Introduction

THE PRECISE measurement of time between two events is the underlying foundation for electronic collimation in positron emission tomography (PET). In a PET system, a positron emitting radionuclide is injected into the patient and when the ejected positron comes into contact with an electron, the two particles annihilate producing two 511 keV gamma rays that are emitted in opposite directions, impacting almost simultaneously the gamma detectors placed around the body. A PET projection image is elaborated by identifying these time coincident pairs of co-linear 511 keV gamma rays among the noise of non-coincident single events impinging the detectors [1].

Assigning a time stamp to the scintillation pulse is not a trivial task due to the time scale being handled and for an optimal performance the system may require periodic calibrations [2]. The classical approach to time discrimination relies on an mixed-signal application specific integrated circuit (ASIC) device designed to yield nanosecond timing accuracy [3-5]. However in preclinical PET systems targeted to small animals a solution based on digital processing of the sampled signal may represent a reasonable trade-off between cost and performance [6, 7].

This work presents and compares different alternatives to the design of a FIR filter that enables accurate real-time estimation of the time stamp based on the sampled energy pulse. In all cases the filtered signal presents an abrupt transition whose zero crossing is related in some sense with the time of occurrence of the detected signal. The motivation to this solution is to provide a direct implementation of a time stamping hardware module that is to be implemented in a field programmable gate array (FPGA), capable of sustaining high count data rates.

The document is structured as follows: the first section summarizes the different timing methods that will be considered and the next presents the material required for the acquisition and processing of the experimental data. Next the result of applying the different filters to the experimental data will be presented, showing that with the proposed filtering approach a event time stamp resolution as low as 1.0 ns FWHM may be achieved for LGSO pulses at a sampling frequency of 65MHz, although the actual figure varies significantly with the scintillation crystal, the sampling frequency and filter type.

II. Timing Filters

A. Constant Fraction Discriminator

The simplest solution to digital timing is implementing the digital equivalent of the constant fraction discriminator (CFD), as shown in equation 1, which is by far the most popular approach to timing in nuclear applications and whose main characteristic is the maintenance of a constant timing edge, since it is not affected by the input pulse amplitude. Its principle of operation is as follows, the analogue signal is split into two components, one of them is delayed *D* and the other is attenuated by the factor *CF*, operations that are implemented with an attenuator and an analogue delay line. Afterwards, these two signals are re-mixed and a comparator detects the zero-cross point, which determines the signal timing.

$$h(t) = \delta(t - D) - CF \cdot \delta(t)$$
$$h[n] = \delta\left[n - \frac{D}{T_s} \right] - CF \cdot \delta[n] \quad (1)$$

When it comes to implementing a non-integer digital delay D/T_s several solutions exist, depending on the selected minimization criteria for the interpolation filter, whose ideal frequency response is:

Manuscript received October 25, 2006. This work has been partially funded by the Spanish Ministry of Culture and Science through the FPU grant program as well as projects TEC2004-07052-C02-02 and PI052204..

P. Guerra, J. E. Ortuño, G. Kontaxakis, M. J Ledesma-Carbayo and A. Santos are with the Electronic Engineering Department, ETSIT, Universidad Politécnica de Madrid, Spain E-20040, (e-mail: pguerra, juanen,gkont, mledesma,andres@die.upm.es).

J.J.Vaquero and M.Desco are with the Hospital General Universitario "Gregorio Marañón", Madrid, Spain E-28007 (e-mail: juanjo, desco@mce.hggm.es).

$$H(e^{j\omega}) = e^{j\omega\frac{D}{T_s}} = e^{j\omega D'} \tag{2}$$

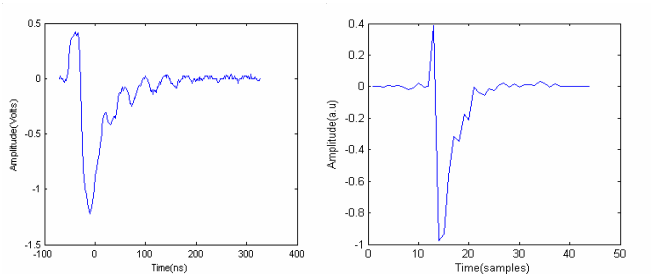

Figure 1: Pulse output of the CFD with an analogue delay of 15 ns and a constant fraction of 0.3 and output of the digital CFD for the same pulse sampled at 60MHz, with an equivalent delay of 15 ns and a constant fraction of 0.3

The most simple and direct approximation comes out of computing and truncating the inverse Fourier transform of the ideal frequency response (2), which results in a shifted and sampled version of the sinc function:

$$e^{j\omega D'} \xleftrightarrow{F} \frac{\sin(\pi(n-D'))}{\pi(n-D')} \quad -\infty < n < \infty \tag{3}$$

In order to produce realizable fractional delay filters, some windowed *w[n]* finite length approximation has to be used. Under these considerations, the digital CFD is expressed in terms of a digital FIR filter *h[n]* as:

$$h[n] = \frac{\sin(\pi(n-D'))}{\pi(n-D')} \cdot w[n] - CF \cdot \partial[n] \tag{4}$$

The time stamp of the pulse *p[n]* is taken as the sample value where the filtered signal crosses the zero level, that is:

$$\hat{\tau} = \arg_n \{p[n] * h[n] = 0\} \tag{5}$$

B. Linear Interpolation

Signal linear interpolation may also be used for the computation of the pulse start point, based on the assumption that the rising edge may be linearly approximated. Despite its simplicity, this approach has proven to be accurate enough for the computation of the time stamp with LSO pulses shaped for 75 ns rise time and sampled at 40 MHz [8] and for LSO/LGSO integrated signals sample at 45MHz [9].

The linear interpolator, in the simplest case, takes into account two samples adjacent to the desired point. In this case, the sample *m* with the steepest slope in the vicinity of the rise edge is taken for the calculation of the line that passes through *m* and *m+1*, and the zero crossing of the interpolated line with the base level is computed as shown in equation (6).

$$\begin{aligned} m &= \arg_n \max\{p'[n]\} \\ \hat{\tau} &= \arg_n \{\hat{p}_m[n] = 0\} \end{aligned} \tag{6}$$

C. Classical Matched Filter

Another possible approach to timing is based on the correlation between the sampled pulse and a template of the reference pulse. In this situation, the criterion is that the timing of the pulse is the point where correlation is maximum. This can be formulated in terms of a FIR filter *h[n]*:

$$\begin{aligned} h[n] &= \frac{A}{\tau_F - \tau_R}\left(\exp^{-\frac{n\cdot T_s}{\tau_F}} - \exp^{-\frac{n\cdot T_s}{\tau_R}}\right) \\ h'[n] &= \frac{A\cdot T_s}{\tau_F - \tau_R}\left(-\frac{\exp^{-\frac{n\cdot T_s}{\tau_F}}}{\tau_F} - \frac{\exp^{-\frac{n\cdot T_s}{\tau_R}}}{\tau_R}\right) \end{aligned} \tag{7}$$

$$\begin{aligned} \hat{\tau} &= \arg_n \max \{p[n] * h[n]\} \\ \hat{\tau} &= \arg_n \{p[n] * h'[n] = 0\} \end{aligned} \tag{8}$$

where *h'[n]* is the first derivative of the impulse response and the time stamp is computed as the point where the filtered *p[n]* crosses the zero level.

D. Optical Matched Filter

The concept of optically matched filter comes, the same way the matched filter does, from communications theory [10]. This approach defines a family of optimal linear filters for filtered Poisson processes detection under Gaussian noise. The formulation takes into account the statistical properties and uncertainties of the signal being detected [10] and was firstly proposed for timing in PET in [11].

The design concept starts with the definition of an inhomogeneous Poisson process $N \equiv \{N(t): t \in [0,T]\}$ with intensity function $\{\lambda(t-\tau): t \in [0,T]\}$, which is decomposed into signal and Poisson noise contributions

$$\begin{aligned} \lambda(t) &= \lambda_s(t) + \lambda_O \\ \lambda_s(t) &= \frac{A}{\tau_F - \tau_R}\left(\exp^{-\frac{t}{\tau_F}} - \exp^{-\frac{t}{\tau_R}}\right) \end{aligned} \tag{9}$$

The observed signal is the sum of a filtered Poisson process and Gaussian noise

$$X(t) = \sum_{i=1}^{N(t)} p(t - t_i) + w(t) \tag{10}$$

where *p(t)* is a known continuous and square-integrable function that represents the detector response to the individual photon. Under these definitions the linear estimator for the timing results from maximization of the expression:

$$\begin{aligned} \hat{\tau} &= \arg_n \max\{p[n] * h[n]\} \\ \hat{\tau} &= \arg_n \{p[n] * h'[n] = 0\} \end{aligned} \tag{11}$$

where *h[n]* is a function of the underlying parameters. The actual value of *h[n]* depends on the selected member of the optical matched filter family, being the simplest case the given by:

$$h(t)=\frac{\lambda(-t)}{\lambda(-t)+\lambda_o+\frac{N_o}{2}} \qquad (12)$$

where $\lambda(t)$ is the reference pulse shape, λ_o is the dark current intensity and *No* is the noise power spectral density.

III. MATERIAL

The experimental data have been obtained with a reengineered version of the LGSO/GSO phoswich detector originally developed for the NIH ATLAS [12], whose energy dynode has been sampled at 625 MHz (Ts=1.6 ns) with a TDS5054B digital oscilloscope (Tektronix, Beaverton, OR, USA). The acquired data has been processed and analyzed with Matlab 6.5 R13 (The Mathworks, Natick, MA, USA).

IV. RESULTS

Up to 10.000 LGSO scintillation pulses were recorded with the oscilloscope and each of them was subsampled by a factor between 5 and 15 with a variable offset, in order to generate a set of pulses at different sampling frequencies with a known relative phase.

The presented timing algorithms have been applied to each subsampled and delayed version of the original pulse and the error between the generated timestamp and the expected result has been recorded. This procedure is based on the fact that, albeit the actual start point of each pulse is unknown, the different samples of the original pulse are spaced by Ts=1.6 ns, therefore the timing estimator is expected to grow linearly with the known delay. As an example Figure 2 (right) shows the behaviour of the matched filter and optically match filter for a particular pulse (left). As it shown, the estimator fluctuates around the expected timing value.

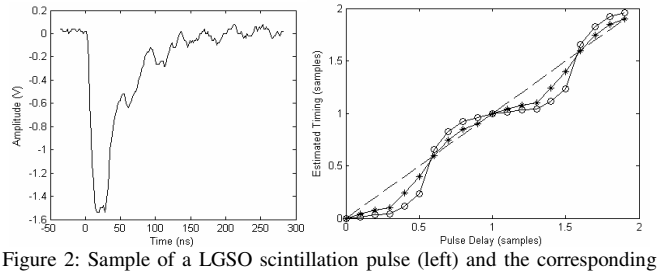

Figure 2: Sample of a LGSO scintillation pulse (left) and the corresponding time estimates vs the introduced delay with the optical filter (*) and the classical matched filter (o) (right).

Repeating this approach for the 10.000 pulses of the set, we have estimated the timing resolution at full width of the half maximum (FWHM) for sampling frequencies ranging between 40 MHz and 125 MHz, as it is shown in Figure 3. It seems obvious that the higher the sampling frequency, the finer the timing resolution. However, as normalized resolution in Figure 3 (right) shows, resolution improvements are not exclusively due to the increasing sampling frequency but also to a better performance of the estimation algorithm, which provides an increasing refinement of the sampling.

One interesting observation is that timing resolution improves as more knowledge about the reference pulse is included, starting from linear interpolation that assumes very little about the reference pulse and ending with the optical filter, that includes shape and noise statistics.

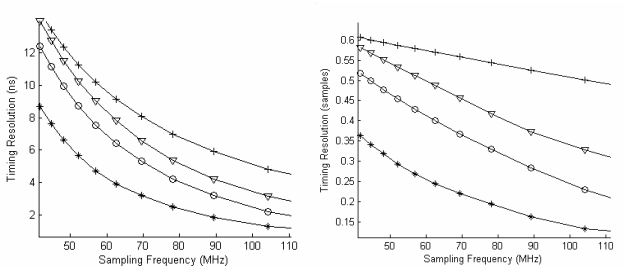

Figure 3: Absolute (left) and normalized (right) singles timing resolution with different algorithms: linear interpolation (+), CFD (▼), matched filter (o) and optical filter (*) for sampling frequencies ranging from 40MHz to 110 MHz.

From a practical point of view, we are particularly interested on the expected timing resolution for sampling frequencies on the 50-80MHz range, where it is feasible to integrate the digital processing electronics into a medium-cost FPGA. Table 1 summarizes results in this range and shows that, within these sampling frequencies, the optical filter outperforms other filter designs.

Table 1: Timing resolution (FWHM) in the frequency range of interest

Filter Type	Resolution (ns) @ 50 MHz	Resolution (ns) @ 65 MHz	Resolution (ns) @ 80 MHz
Linear	11.80	8.71	6.77
CFD	10.82	7.32	5.11
Match	9.33	5.97	4.02
Optical	6.12	3.61	2.34
Optical (calibr)	4.75	2.52	1.55

As it is observed in Figure 2 (right), timing estimators introduce systematic errors which can be estimated and compensated based on the acquired data, without any previous calibration. As a result of this compensation, the timing resolution of the optical filter is even further reduced, as it is shown in Table 1 and Figure 4.

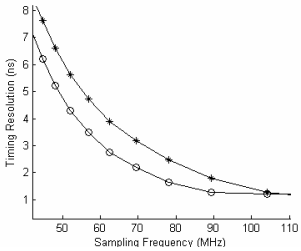

Figure 4: Optical Filter after self-calibration.(o) versus the non-corrected results (*).

Results summarized in these plots are compatible with those presented by other authors in [6, 7, 13, 14], although the latter represent single points of the much wider design space covered in this work.

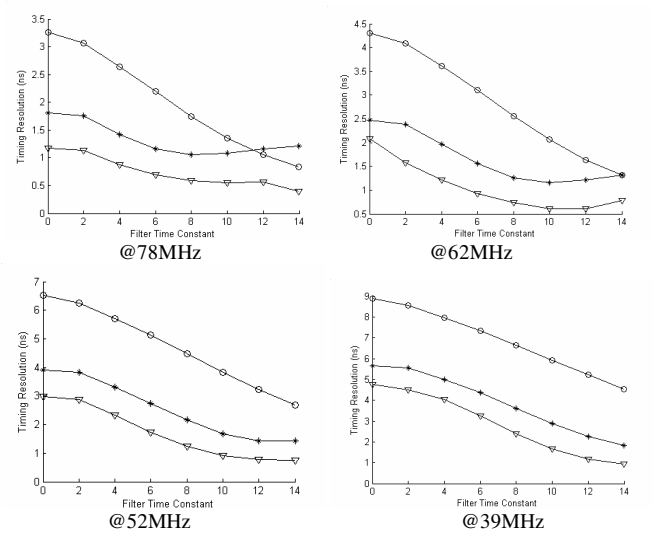

Figure 5: Self-calibrated optical filter (▼), non-calibrated optical filter (*) and matched filter (o) for sampling frequencies of 78 MHz (up-left), 62 MHZ (up-right), 52 MHz (bottom-left) and 39 MHZ (bottom-right) with shaping constants between 0 and 14 ns.

Although it is commonly accepted that the lower the rise time of the scintillation pulse the better the time resolution, when it comes to timing by digital means some smoothing is required in order to capture more samples from the rising edge. Therefore we have also analyzed the benefits of further shaping the energy signal pulse, whose measured rising time is 10 ns, before sampling. A Gaussian filter of variable time constant is applied to the same data set, before applying the timing algorithms hereinbefore described. Figure 5 shows the benefits of a slight increase on the signal rise time, that will introduce no significant change in the acquisition dead time and which additionally may provide some improvements regarding energy estimation. These results suggest when the proper smoothing is select that in all cases it is possible to achieve single timing resolutions below 1.0 ns (FHWM), even with modest sampling frequencies, when the proper filter and shaping time is selected.

V. Conclusions

This work analyzes the expected resolution of the time stamp when computed by digital means for LGSO pulse with a nominal rise time of 10 ns and decay time of 40 ns. Different FIR filters are considered for the analysis; all of them derived from the two exponentials model, which is suitable to describe pulses from most scintillators. This model based approach has the advantage of not requiring previous pre-processing or calibration in order to compute the adequate filter response.

In all cases the time stamp is computed after filtering the input energy signal and finding its zero crossing through interpolation. The motivation to a solution of this type versus other more elaborated solutions is that FIR filtering and dividing are common operations in signal processing that are easily and efficiently implemented on programmable hardware, enabling direct real-time computation of the time stamp.

Filter performance has been analyzed for a wide range of sampling frequencies and it has been shown that, in the sampling rate of interest (around 40-100MHz), results are promising, as most of them provide enough resolution for the application of a 10 ns timing window and in the particular case of the optically matched filter it seems feasible to apply a 5 ns timing window.

However we must be aware that the presented results are applicable to a single detector and neglect fixed point effects as well as timing variations due to component and clock jitter among several detectors in the ring. Some of these uncertainties may be compensated by calibration and some will not, and the impact of these on timing resolution is open for further investigation.

Acknowledgments

The authors thank SUINSA Medical Systems Engineering Department for providing the detector that was used to acquire the experimental data.

References

[1] G. Kontaxakis, "Positron Emission Tomography," in *Encyclopedia of Medical Devices and Instrumentation*, vol. 5, 2nd ed. New Jersey: John Wiley & Sons, 2006, pp. 406-418.

[2] C. J. Thompson and A. L. Goertzen, "A Method for Determination of the Timing Stability of PET Scanners", *IEEE Transactions on Medical Imaging*, vol. 24, pp. 1053-1057, 2005.

[3] E. Raisanen-Ruotsalainen, *et al.*, "An integrated time-to-digital converter with 30-ps single-shot precision", *IEEE Journal of Solid-State Circuits*, vol. 35, pp. 1507-1510, 2000.

[4] P. Dudek, *et al.*, "A high-resolution CMOS time-to-digital converter utilizing a Vernier delay line", *IEEE Journal of Solid-State Circuits*, vol. 35, pp. 240-247, 2000.

[5] B. K. Swann, *et al.*, "A 100-ps time-resolution CMOS time-to-digital converter for positron emission tomography imaging applications", *IEEE Journal of Solid-State Circuits*, vol. 39, pp. 1839-1852, 2004.

[6] A. Mann, *et al.*, "A sampling ADC data acquisition system for positron emission tomography," at *IEEE Nuclear Science Symposium*, vol. 1, pp. 296-300, Rome, 2004.

[7] G. Hegyesi, *et al.*, "Ethernet Based Distributed Data Acquisition System for a Small Animal PET," at *IEEE-NPSS Real Time Conference*, pp. 275-279, Stockholm, 2005.

[8] M. Streun, *et al.*, "Coincidence detection by digital processing of free-running sampled pulses ", *Nuclear Instruments and Methods in Physics Research Section A*, vol. 487, pp. 530-534, 2002.

[9] R. Fontaine, *et al.*, "The architecture of LabPET, a Small Animal APD-based Digital PET Scanner," at *IEEE Nuclear Science Symposium*, pp. 2785-2789, Puerto Rico, 2005.

[10] E. Geraniotis and H. Poor, "Robust Matched Filters for Optical Receivers", *IEEE Transactions on Communications*, vol. 35, pp. 1289-1296, 1987.

[11] A. O. Hero, III, "Timing estimation for a filtered Poisson process in Gaussian noise", *IEEE Transactions on Information Theory*, vol. 37, pp. 92 - 106, 1991.

[12] J. Seidel, *et al.*, "Resolution uniformity and sensitivity of the NIH ATLAS small animal PET scanner: Comparison to simulated LSO scanners without depth-of-interaction capability", *IEEE Transactions on Nuclear Science*, vol. 50, pp. 1347-1350, 2003.

[13] J.-D. Leroux, *et al.*, "Time discrimination techniques using artificial neural networks for positron emission tomography," at *IEEE Nuclear Science Symposium*, vol. 4, pp. 2301-2305, Rome, 2004.

[14] E. Albuquerque, *et al.*, "Performance Simulation Studies of the Clear-PEM DAQ/Trigger System," at *IEEE-NPSS Real Time Conference*, pp. 151-155, Stockholm, 2005.